Naval Research Laboratory
Stennis Space Center, MS 39529-5004

NRL/FR/7322--93-9429

Hindcasting Changes in Thermal Structure and Acoustic Transmission Loss in the Upper Ocean on Short Time Scales with Data from MILE and from Ocean Weather Station Papa

PAUL J. MARTIN

Ocean Sciences Branch
Oceanography Division

January 18, 1995

REPORT DOCUMENTATION PAGE

Form Approved
OBM No. 0704-0188

1. AGENCY USE ONLY *(Leave blank)*	2. REPORT DATE	3. REPORT TYPE AND DATES COVERED
	January 18, 1995	Final

4. TITLE AND SUBTITLE
Hindcasting Changes in Thermal Structure and Acoustic Transmission Loss in the Upper Ocean on Short Time Scales with Data from MILE and from Ocean Weather Station Papa

5. FUNDING NUMBERS

Job Order No.	573508804
Program Element No.	0602435N
Project No.	RM35G95
Task No.	801
Accession No.	DN256002

6. AUTHOR(S)
Paul J. Martin

7. PERFORMING ORGANIZATION NAME(S) AND ADDRESS(ES)
Naval Research Laboratory
Oceanography Division
Stennis Space Center, MS 39529-5004

8. PERFORMING ORGANIZATION REPORT NUMBER
NRL/FR/7322--93-9429

9. SPONSORING/MONITORING AGENCY NAME(S) AND ADDRESS(ES)
Office of Naval Research
ONR Code 120M
800 N. Quincy Street
Arlington, VA 22217-5000

10. SPONSORING/MONITORING AGENCY REPORT NUMBER

11. SUPPLEMENTARY NOTES

12a. DISTRIBUTION/AVAILABILITY STATEMENT
Approved for public release; distribution unlimited.

12b. DISTRIBUTION CODE

13. ABSTRACT *(Maximum 200 words)*

The skill of mixed-layer hindcasts of short (less than 5 d) duration was investigated using data from Ocean Weather Station Papa for the years 1960 to 1968, and with data from the Mixed-Layer Experiment (MILE), which was conducted about 40 km southwest of Papa in late summer of 1977. The hindcasts were initialized and validated with observed temperature profiles and forced with surface wind stresses and heat fluxes calculated from meteorological observations. Mean and rms hindcast errors for sea-surface temperature (SST), mixed-layer depth (MLD), surface sound-channel depth (SCD), and acoustic-detection range (ADR) were compared with errors for persistence and climatology. Hindcast skill was calculated as the percent improvement of the hindcast rms error over the persistence rms error.

The hindcast skill was significantly higher for the MILE data than for the Papa data, and hindcast skill with the Papa data was generally higher in spring and summer than in fall and winter. The range of hindcast skill for hindcasts of 12- and 36-h duration was 39 to 48% for SST, 28 to 37% for MLD, and 38 to 43% for SCD for the MILE data versus 14 to 19% for SST, 22 to 33% for MLD, and 8 to 31% for SCD for the Papa data for the spring and summer. Smoothing the MILE temperature observations with a 2-h running mean resulted in an increase in hindcast skill of about 3% due to the reduction in small-scale noise.

The persistence rms MLD error was found to exceed the climatological error after about 2 d for both the MILE and the Papa hindcasts for spring and summer, a result that illustrates the high variability and short correlation time of MLD at this time of year. Additionally, hindcasts initialized from climatology in spring and summer showed skill for MLD similar to that for hindcasts initialized from an observed profile for hindcast durations longer than about 2 d. This result demonstrates that the near-surface thermal stratification

14. SUBJECT TERMS
tactical scale models, ocean models, acoustic models

15. NUMBER OF PAGES
26

16. PRICE CODE

17. SECURITY CLASSIFICATION OF REPORT	18. SECURITY CLASSIFICATION OF THIS PAGE	19. SECURITY CLASSIFICATION OF ABSTRACT	20. LIMITATION OF ABSTRACT
Unclassified	Unclassified	Unclassified	Same as report

of climatological estimates of thermal structure can be improved by mixed-layer hindcasts, since the hindcasts allow the profiles to adjust to recent atmospheric forcing.

Hindcast and persistence errors for ADR (defined as the range at which the transmission loss first exceeds 80 dB) were calculated for the MILE data with both the Parabolic Equation (PE) and Passive Raymode acoustic models for frequencies of 1000, 2000, and 4000 Hz for a source and receiver depth of 10 m. The range of hindcast skill for ADR for hindcasts of 12- and 36-h duration was 22 to 44% for the PE model and 2 to 38% for Passive Raymode. ADR errors were calculated for the Papa data with Passive Raymode for frequencies of 250, 1000, and 4000 Hz for a source and receiver depth of 20 m. As for SST, MLD, and SCD, the skill for hindcasts of ADR with the Papa data was generally higher in the spring and summer than in the fall and winter, and lower than the comparable calculations made with the MILE data.

The calculation of hindcast skill for ADR with the MILE and Papa data showed a general decrease in skill as the depths of the source and receiver were increased. Comparisons of skill in hindcasting ADR determined from transmission loss calculations with the Passive Raymode and PE acoustic models showed more consistent results with the PE model, especially for cases where the upper-ocean ducting was marginal or the source and receiver were below 30 m.

CONTENTS

HINDCASTING CHANGES IN THERMAL STRUCTURE AND ACOUSTIC TRANSMISSION LOSS IN THE UPPER OCEAN ON SHORT TIME SCALES WITH DATA FROM MILE AND FROM OCEAN WEATHER STATION PAPA

I. INTRODUCTION

This study is part of an ongoing investigation of the skill of short-duration hindcasts of the thermal structure of the upper ocean with mixed-layer models, and the effect of the hindcast changes in upper-ocean thermal structure on acoustic prediction. Martin (1989) looked at the skill of mixed-layer hindcasts of 24-h duration in predicting the near-surface thermal structure at Ocean Weather Station (OWS) Papa for the year 1961. Martin (1989) also looked at the skill of 12- to 48-h mixed-layer hindcasts that used data from the Mixed-Layer Experiment (MILE), which was conducted near Papa in late summer of 1977. Martin (1993) investigated the effect of 12- to 48-h mixed-layer hindcasts on the prediction of thermal structure and acoustic transmission loss with the Papa data from 1961. The acoustic calculations were made with the Passive Raymode acoustic model for frequencies between 100 and 8000 Hz for a source and receiver at 20-m depth. Martin (1994) did a similar study with data from OWSs November, Papa, and Victor for data that covered a period of several years.

All of these studies utilized the Mellor-Yamada Level 2, Garwood, and Price mixed-layer models. Hindcast skill was investigated for sea-surface temperature (SST), mixed-layer depth (MLD), surface or near-surface sound-channel depth or thickness (SCD), and acoustic detection range (ADR). ADR for a given frequency is defined as the range at which the transmission loss at that frequency first exceeds 80 dB. Ocean Stations November and Papa are in the northeast Pacific at 30° N, 140° W and 50° N, 145° W, respectively, and Victor is in the northwest Pacific in the path of the Kuroshio Extension at 34° N, 164° E.

The hindcasts with the ocean station data (Martin 1994) generally showed skill over persistence, but the skill levels were not very high. For the spring and summer seasons, the hindcast skill for MLD relative to persistence (for 12-h hindcasts) was 12 to 23% at November, 19 to 24% at Papa, and 4 to 12% at Victor. For SST the skill levels were lower: –3 to 7% at November, 10 to 14% at Papa, and –1 to 2% at Victor. The skill levels for ADR were roughly similar at the three stations, with a range for the spring and summer of 5 to 15% for a frequency of 1000 Hz, and 3 to 12% for a frequency of 4000 Hz.

Skill levels with data from MILE (Martin 1989), however, were significantly higher: 39 to 44% for SST and 33 to 46% for MLD for 12-h hindcasts. Since MILE was conducted near Papa, the MILE results can be compared with those for Papa during late summer. The higher levels of hindcast skill with the MILE data were attributed to better data—primarily to more accurate ocean temperature measurements. An indication of the greater accuracy of the MILE temperature observations is that the hindcast skill for SST and MLD with the MILE data was similar, whereas for the Papa data the hindcast skill for SST was significantly lower than for MLD.

The purposes of the present study are to perform a more detailed comparison of hindcast skill for SST, MLD, SCD, and ADR with the MILE and Papa data, and to answer some questions that have not been previously addressed:

• How does the climatological error for upper-ocean thermal structure compare with the error for persistence and for mixed-layer hindcasts, and how long does it take for the persistence error to exceed the climatological error?

• What is the error for a hindcast initialized from climatology instead of from an observed temperature profile, i.e., can mixed-layer hindcasting improve the near-surface thermal stratification of climatological estimates of thermal structure?

• What is the effect of temporal smoothing of the MILE temperature data on hindcast skill? It would be expected that the smoothing of short-time-scale variability in the temperature data would tend to reduce the persistence and hindcast errors and improve hindcast skill.

• What is the hindcast skill for ADR with the MILE data, and how does it compare with that for the Papa data at the same time of year? Since previous calculations of hindcast skill for SST, MLD, and SCD with the MILE data were higher than the corresponding calculations with the OWS data, it is expected that hindcast skill for ADR will also be higher with the MILE data.

• How do hindcast errors for ADR calculated with the Passive Raymode acoustic model compare with ADR errors calculated with a parabolic equation (PE) model with the data from MILE? Previous calculations of the hindcast skill for ADR at the ocean stations utilized the Passive Raymode model because of its much greater efficiency and the large number of transmission loss calculations that had to be made. The PE model, however, can provide more accurate calculations of transmission loss, and because there are far fewer transmission-loss calculations needed with the MILE data than with the OWS data, efficiency is of less concern.

• What is the effect of changing the depth of the source and receiver on the calculation of hindcast skill for ADR with the MILE and Papa data? Previous calculations of hindcast skill for ADR at the ocean stations were for a source and receiver located at 20 m. This shallow depth was selected to obtain a high sensitivity of transmission loss to changes in thermal stratification caused by atmospheric forcing. The investigation of other depths for the source and receiver will provide results for a greater variety of situations, e.g., cross-duct propagation.

The following sections include (II) a description of the mixed-layer model used for the hindcasts, (III) a discussion of the MILE and Papa data, (IV) a calculation of a climatology for upper-ocean thermal structure at Papa, (V) a presentation of the hindcast results for upper-ocean thermal structure, (VI) a presentation of the hindcast results for acoustic detection range, (VII) a summary, and (VIII) conclusions.

II. THE MIXED-LAYER MODEL

The Price mixed-layer model was used for the mixed-layer hindcast results presented here. In previous studies (Martin 1989, 1993, 1994), the Price, Mellor-Yamada Level 2 (MYL2), and Garwood mixed-layer models were compared and found to give roughly similar errors for hindcasts of SST, MLD, and ADR with data from Papa and MILE. Hence, the results obtained here with the Price model should be indicative of results that would be obtained with the other two models. Only a brief description of the Price model is provided here. For more detail, see Price et al. (1986).

As with most other mixed-layer models, the Price model utilizes the mean equations for the conservation of heat, salt, and momentum in the vertical. The model is initialized by providing initial profiles of temperature, salinity, and Ekman velocity, and is forced by times series of the surface fluxes of heat, salt, and momentum. Advection and horizontal diffusion are ignored in the single-station simulations conducted here, and vertical transport is due only to turbulent mixing.

The calculation of vertical mixing for the Price model proceeds in two steps. First, the surface mixed layer is deepened based on a bulk Richardson number criteria in the manner of Pollard et al. (1973). Within this layer heat, salt, and momentum are completely mixed. Then, the density and momentum gradients that form the base of the mixed layer are diffused according to a local Richardson number criteria, a process that has been referred to as "turbulent adjustment" (Stull and Hasegawa 1984). An advantage of the Price model over most bulk mixed-layer models is that the process of turbulent adjustment provides a smooth transition in the profiles at the base of the mixed layer, rather than the sharp discontinuity that is characteristic of most bulk models. Because the mixing depends on a Richardson number criteria, the Price model has a behavior similar to that of the MYL2 and other eddy-coefficient models in which mixing depends on a local Richardson number (Kundu 1980; Martin 1986). An advantage of the Price model and most bulk models, with respect to eddy-coefficient models, is that a larger timestep can be used. Eddy-coefficient models require a relatively small timestep to maintain the accuracy and stability of their vertical diffusion terms.

Below the mixed layer, vertical turbulent mixing occurs intermittently due to shear instability, breaking internal waves, and other processes. Based on Martin (1985), the value used for ambient vertical diffusion below the mixed layer for heat, salt, and momentum was 0.02 cm^2/s.

The model equations were solved numerically on a stretched vertical grid with a resolution at the surface of 2 m and a 3% increase in the thickness of each layer with depth. The timestep used was 1800 s.

III. PAPA AND MILE DATA

A. Papa Data

Ocean Station Papa is located in the northeast Pacific at 145° W, 50° N. Papa was maintained as a Canadian weathership station from the 1940s until 1981. The weatherships that occupied Papa collected both meteorological data and ocean bathythermograph (BT) observations on a regular schedule. For this study we used data from the beginning of 1960 to the end of 1968.

Between 1960 and 1979, BTs are generally available at Papa at least twice a day at 0200 and 1700 GMT; however, the frequency of the BT observations and the times at which they were taken are subject to considerable variability. Up until the 1970s, the observations at Papa were taken mostly by mechanical BTs (MBTs). In 1968 expendable BTs (XBTs) began being taken, and in 1974 the MBTs were phased out. The BT data used here were taken between 1960 and 1968 and are primarily MBTs. These data consist of temperature values recorded every 5 m from the surface to about 275 m. The BT data were edited to remove obviously bad and unusable profiles. The total number of BTs in the 9 yr of data that were used was 14,688, which is an average of about 4.5 BTs/d.

Meteorological observations were taken at Papa every 3 h. Between 1960 and 1968 very few gaps are present in this data, and the gaps that exist are short. Missing and obviously erroneous meteorological data, i.e., values differing greatly from neighboring values, were filled in by linear

(temporal) interpolation. The meteorological observations include windspeed and direction, SST, air and dew point temperature, air pressure, and cloud cover.

Surface wind stress and heat flux at Papa were calculated from the meteorological observations using standard formulas. Windspeed was reduced 7% to correct to 10-m height. The windspeed-dependent drag coefficient of Garratt (1977) was used to calculate wind stress, and a coefficient of 0.00167 was used to calculate latent and sensible heat exchange. Both coefficients were corrected for stability (Kondo 1975). The Berliand (Wyrtki 1965) formula was used to calculate net longwave radiation. Solar insolation was calculated using the Fritz clear-sky formula (List 1958) along with the Tabata (1964) cloud correction. Tabata's formula for the attenuation of solar radiation by clouds was derived from radiation measurements made at Papa from 1959 through 1961. The surface albedo was taken to be 6%, and the extinction profile of Jerlov (1976) for optical type II seawater was used to parameterize the extinction of solar radiation with depth.

Tables 1 and 2 list the monthly averaged values of wind stress and heat flux calculated from the meteorological observations from 1960 to 1968. The wind stress at Papa is strong in fall and winter with an average value of about 3 dynes/cm^2. Strong wind events occur every few days as weather systems pass through. Between June and August the winds are weaker and wind events are less frequent. The average wind stress during the summer was calculated to be about 1 dyne/cm^2.

B. MILE Data

MILE took place about 40 km southwest of Papa between 19 August and 8 September 1977 (Davis et al. 1981). The experiment was conducted specifically to investigate the response of the mixed layer to atmospheric forcing. Subsurface moored instruments spaced at 3-m intervals beginning at 5-m depth were used to measure temperature and velocity every 112.5 s. The high frequency of the subsurface observations allows the data to be filtered to eliminate high-frequency variability.

Table 1 — Monthly Mean Surface Wind Stress and Heat Flux at Papa Calculated from Meteorological Observations for 1960 through 1968

	Wind Stress (dynes/cm^2)			Heat Flux (ly/d)				
Month	Mag	E–W	N–S	Solar	Back	Latent	Sensible	Total
Jan	3.02	0.90	0.48	57	–101	–101	–22	–168
Feb	2.70	0.95	0.76	105	–98	–75	–7	–76
Mar	2.64	1.05	–0.38	190	–106	–121	–32	–69
Apr	2.13	1.15	–0.06	307	–103	–103	–16	85
May	1.50	0.60	0.11	378	–89	–55	4	238
Jun	1.11	0.49	0.26	396	–78	–37	8	289
Jul	0.82	0.38	0.13	362	–71	–27	5	268
Aug	1.23	0.68	0.19	301	–76	–58	4	170
Sep	1.76	0.88	0.49	230	–91	–95	0	45
Oct	3.26	1.94	0.38	144	–115	–204	–41	–216
Nov	3.85	1.88	0.06	75	–114	–178	–44	–261
Dec	3.19	0.95	0.10	48	–110	–129	–42	–232
Avg	2.27	0.99	0.21	216	–96	–99	–15	6

Table 2 — Monthly Climatological Near-Surface Thermal Stratification at Papa Calculated from the BTs and from the Monthly Mean Temperature Profiles. The Thermal Stratification is Defined in Terms of the Depth at which the Temperature Becomes Less Than the SST by an Amount dT. The Depths Listed are in Meters.

dT (°C)	Jan	Feb	Mar	Apr	May	Jun	Jul	Aug	Sep	Oct	Nov	Dec
Mean Stratification from BTs												
0.1	93	79	70	51	30	19	15	19	29	46	64	90
0.2	107	105	99	68	39	23	18	22	32	51	69	98
0.3	112	120	118	87	47	26	20	24	34	53	72	101
0.4	115	126	126	96	52	28	22	25	35	54	74	102
0.5	117	131	133	104	57	29	23	26	36	54	74	103
0.6	119	135	142	113	62	31	25	27	37	54	75	104
0.7	121	140	150	121	67	33	26	28	38	55	76	105
0.8	123	146	158	131	74	34	27	29	38	55	76	106
0.9	126	152	164	138	79	36	27	29	38	55	76	107
1.0	129	158	171	145	84	37	28	30	39	56	77	108
Stratification from Monthly Mean Temperature Profiles												
0.1	88	91	64	34	16	11	9	11	22	39	56	85
0.2	92	103	92	62	27	16	14	17	27	41	59	89
0.3	96	110	108	83	35	19	17	21	30	42	61	92
0.4	100	117	121	94	42	22	20	22	31	43	62	94
0.5	106	123	129	102	47	24	21	24	32	44	63	96
0.6	113	129	136	107	53	26	23	25	33	45	65	98
0.7	119	135	143	113	58	28	24	26	33	46	66	101
0.8	124	141	150	118	64	30	25	26	34	46	67	103
0.9	128	147	157	124	69	32	26	27	35	47	68	105
1.0	132	154	164	131	75	34	26	28	35	48	69	107

Temporal filtering of the temperature data was performed for some of the experiments to investigate the effect of such filtering on hindcast skill.

Note that the SST referred to for the MILE data is actually the temperature at 5-m depth, since this was the shallowest temperature that was observed. The MLD is defined as the depth at which the temperature is 0.2°C below the 5-m temperature. The uppermost temperature being at a depth of 5 m causes some error in determining the SST and MLD during those times when the mixed layer is near to or shallower than 5 m. However, so that the calculation of SST, MLD, and other properties of the observed and hindcast temperature profiles would be consistent, the temperature profiles from the MILE hindcasts were interpolated to the depths of the observed temperatures before these calculations were made.

Meteorological observations taken every 3 h provide the information needed to estimate surface momentum and heat fluxes during MILE. Wind stress and latent and sensible heat flux were calculated from the meteorological observations using bulk aerodynamic formulas in the same manner as with the Papa data. The solar and longwave radiation during MILE were measured directly every hour.

Figure 1 shows plots of the surface wind stress, the total surface heat flux, and the observed 5-m temperature and MLD during MILE. Figure 1 shows a general warming of the SST between 19 August and 8 September, a diurnal fluctuation of SST and MLD due to diurnal solar heating, and a significant cooling and deepening of the mixed layer on 22–23 August that was caused by a storm.

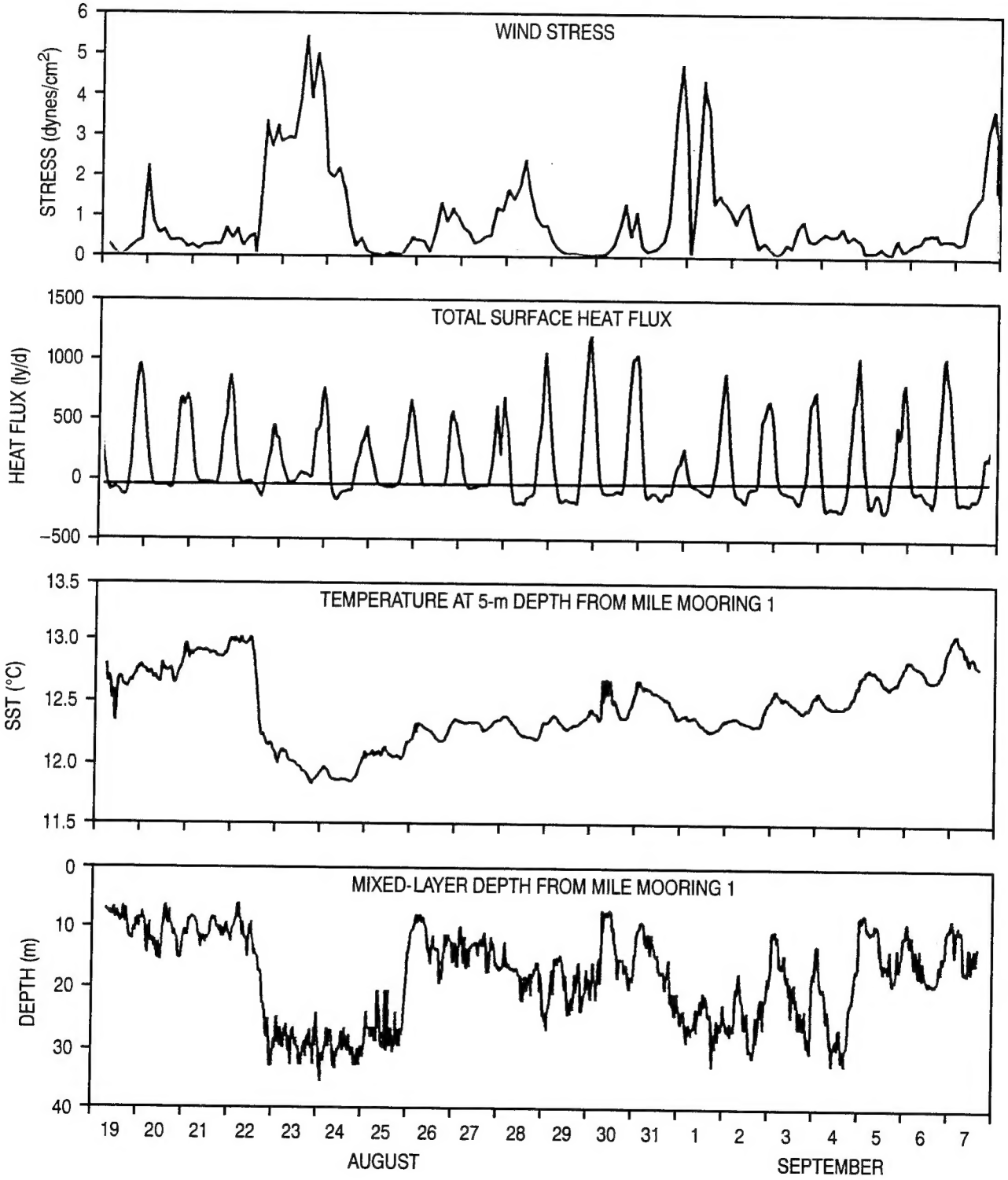

Fig. 1 — The surface wind stress, surface heat flux, 5-m temperature, and MLD during MILE

IV. CALCULATION OF A THERMAL CLIMATOLOGY AT PAPA

A monthly climatology of the upper-ocean temperature field at Papa was calculated by averaging the BT profiles for each month (Fig. 2). A climatology for the near-surface thermal stratification was also determined by calculating the average depth at which the temperature becomes less than the SST by amounts ranging from 0.1 to 1.0°C (Table 2). Note that a common definition of the MLD is the depth at which the temperature becomes 0.1 or 0.2°C less than the SST.

Table 2 also contains the near-surface stratification calculated from the monthly climatological profiles. These stratification depths are generally shallower than those calculated from the actual BTs. This might be expected since averaging BTs together smooths the vertical gradients and, as a result, tends to increase the near-surface stratification and reduce the MLD and surface SCD.

The near-surface stratification of the monthly mean profiles can be adjusted to more accurately represent the climatological near-surface stratification. This was done here by (a) setting the SST to the climatological value, (b) using the climatological stratification from the surface down to the depth where the temperature becomes 0.5°C less than the SST, and then (c) blending the temperature back to the climatological profile over a depth scale of 50 m. The result is a thermal climatology that more accurately reflects the observed near-surface stratification and MLD. The isotherm depths from the modified climatological temperature profiles are plotted in Fig 3. Comparing Fig. 3 with Fig. 2, it can be seen that the modified profiles are in better agreement with the observed mean MLD. The climatological temperature profiles, with their near-surface stratification adjusted as described here, were used to represent the thermal climatology at Papa in the experiments described in this report.

V. RESULTS OF THE HINDCASTS FOR SST, MLD, AND SCD

The hindcasts with the MILE and Papa data were conducted by initializing the Price mixed-layer model with the observed temperature profiles, and by forcing the model with the wind stresses and heat fluxes calculated from the meteorological observations (section III). Salinity was initialized

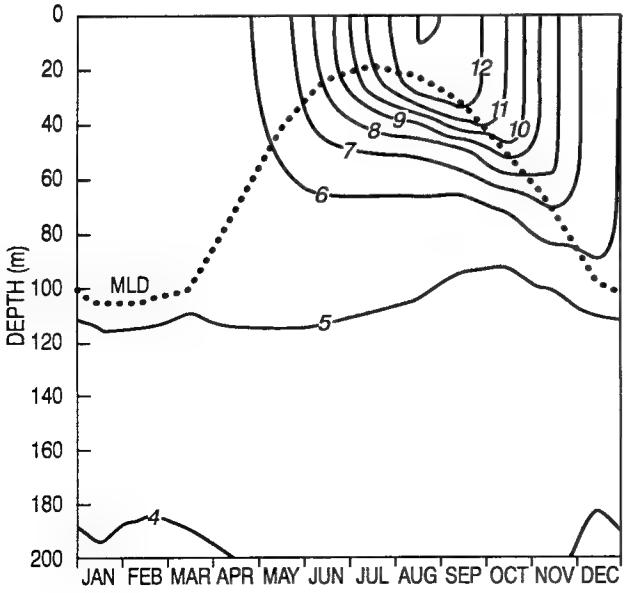

Fig. 2 — The climatological temperature variation in the upper 200 m at Papa interpolated from the monthly climatological temperature profiles. The climatological MLD, calculated as the mean MLD of the individual BTs, is shown as a dotted line.

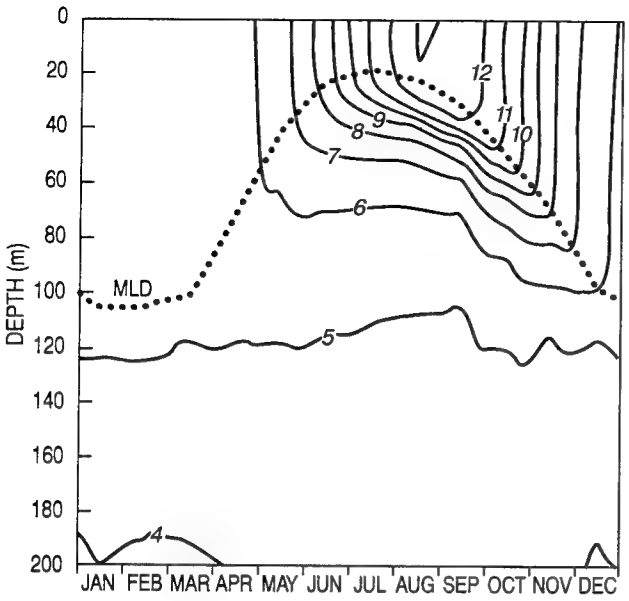

Fig. 3 — As in Fig. 2, but the near-surface stratification of the climatological temperature profiles has been adjusted to better agree with the near-surface stratification of the observed profiles. The climatological MLD, which is calculated as the mean MLD of the individual BTs, is shown as a dotted line. This is the same MLD as is shown in Fig. 2.

from a climatological profile (Beatty 1977) with salinity variations in the upper 80 m (i.e., above the main halocline) eliminated (Martin 1993), and the near-surface, wind-driven Ekman current was initialized to zero. Simulations at Papa have indicated that errors due to the initialization of the salinity and Ekman velocity in this manner tend, on average, to be relatively small (Martin 1988).

The hindcasts were validated by comparing the hindcast temperature profiles with the observed profiles. The hindcast profiles were interpolated to the depths of the observed profiles before making the comparisons. Hindcast errors were calculated for SST, MLD, and SCD. MLD is defined here as the depth at which the temperature becomes 0.2°C less than the SST, and SCD is defined as the depth of the surface sound channel, which is taken to be the depth of the sound speed maximum in the upper 200 m.

Hindcasts were initiated every 3 h with the MILE data, which resulted in about 140 hindcasts being conducted over the 20-d period. The Papa hindcasts were initiated every 3 h if temperature profiles were available for both initialization and validation (within 3 h). A total of about 9000 hindcasts were conducted with the Papa data for the period 1960 to 1968. The purpose of initiating hindcasts every 3 h was to conduct hindcasts during different times of the day and to utilize a fairly large percentage of the available BT profiles.

Table 3 shows a comparison of the errors for the mixed-layer hindcasts with the MILE data with the errors for climatology and persistence. Mean and rms errors are listed for SST, MLD, and SCD for hindcasts of 12-, 24-, 36-, 48-, and 72-h duration for both the unsmoothed temperature data and for the temperature data that were temporally smoothed with a 2-h running mean. The skill shown for the hindcasts is defined as the percent improvement of the hindcast rms error over the persistence rms error.

Hindcast skill with the unsmoothed temperature data is quite good: 39 to 51% for SST, 28 to 37% for MLD, and 38 to 45% for SCD. The hindcast skill improves as the duration of the hindcasts is increased up to about 48 h. There is a slight drop in skill between 48 and 72 h. This may be due to the limited duration of the MILE data and the fact that fewer cases are used to calculate the error statistics as the hindcast duration is increased.

Table 3 — Summary of Mean and rms SST, MLD, and SCD Errors for 12- to 72-h Hindcasts Made with the MILE Data. The Model Hindcast Error is Compared with the Errors for Climatology and Persistence. Model Skill is the Percent Improvement of the Model Hindcast rms Error Over the Persistence rms Error. Results are Shown for Both Unsmoothed and Smoothed MILE Temperature Data.

Hindcast Duration (h)	Model	SST			MLD			SCD		
		Mean (°C)	rms (°C)	Skill	Mean (m)	rms (m)	Skill	Mean (m)	rms (m)	Skill
Results with Unsmoothed Temperature Data										
	Climate	0.52	0.61		8.0	10.8		9.8	12.5	
12	Persistence	−0.01	0.18		−0.2	7.0		−0.1	6.4	
	Hindcast	0.00	0.11	39%	0.4	5.0	28%	1.3	3.9	38%
24	Persistence	−0.01	0.24		−0.2	7.7		−0.1	7.8	
	Hindcast	−0.01	0.15	39%	1.4	5.2	33%	1.8	4.9	38%
36	Persistence	−0.02	0.33		−0.4	9.9		−0.2	9.8	
	Hindcast	−0.01	0.17	48%	2.1	6.3	37%	2.2	5.6	43%
48	Persistence	−0.02	0.37		−0.4	10.3		−0.2	10.5	
	Hindcast	−0.01	0.18	51%	2.9	6.7	34%	2.7	5.7	45%
72	Persistence	0.00	0.43		−0.8	11.8		−0.2	10.9	
	Hindcast	−0.01	0.22	49%	3.8	7.6	35%	3.3	6.6	40%
Results with Temperature Data Smoothed with 2-h Running Mean Filter										
	Climate	0.53	0.62		8.1	10.6		10.7	13.0	
12	Persistence	−0.01	0.18		−0.2	6.4		−0.1	6.0	
	Hindcast	0.00	0.10	43%	0.6	4.3	33%	1.2	3.6	40%
24	Persistence	−0.01	0.24		−0.3	7.1		−0.1	7.6	
	Hindcast	−0.01	0.13	44%	1.5	4.6	36%	2.0	4.5	42%
36	Persistence	−0.02	0.33		−0.4	9.2		−0.2	9.5	
	Hindcast	−0.01	0.16	51%	2.1	5.5	40%	2.3	5.3	44%
48	Persistence	−0.02	0.37		−0.5	10.3		−0.2	10.2	
	Hindcast	−0.02	0.18	52%	2.8	6.0	37%	2.8	5.4	47%
72	Persistence	0.00	0.43		−0.9	10.9		−0.3	10.5	
	Hindcast	−0.02	0.21	51%	3.8	7.1	35%	3.5	6.5	38%

For the hindcasts with the smoothed temperature data, the hindcast skill is 43 to 52% for SST, 33 to 40% for MLD, and 40 to 47% for SCD. The hindcast skill with the smoothed temperature data is slightly higher than with the unsmoothed data as expected. The smoothing eliminates some of the short time-scale variability that the mixed-layer hindcasts do not account for. Even with 2-h smoothing, there remains in the MILE temperature data internal wave motions with a period of several hours

and a peak-to-peak amplitude of about 15 m, which are caused by internal tides (Davis et al. 1981). These low-frequency internal waves contribute to the error in the hindcasts.

Table 4 shows seasonal hindcast results with the Papa data for hindcasts of 12- and 36-h duration. As noted previously (Martin 1994), the hindcast skill is much higher during the heating season in spring and summer than in fall and winter. In spring and summer, the hindcast skill is 14 to 19% for SST, 22 to 33% for MLD, and 8 to 31% for SCD. The hindcast skill steadily improves for SST, MLD, and SCD as the duration of the hindcasts is increased from 12 to 36 h. The hindcast skill with the Papa data during the summer can be compared with the hindcast skill with the MILE data, and it can be seen that the hindcast skill with the Papa data is significantly lower, especially for SST and SCD.

Figure 4 shows rms MLD error versus time for the MILE data for hindcasts of 3- to 120-h duration. Four error curves are plotted: the error of a hindcast initialized from an observed profile, the error of a hindcast initialized from a climatological profile, the error for persistence, and the error for climatology. This figure illustrates a couple of interesting points. One is that the persistence error exceeds the climatological error after about 2 d, i.e., climatology provides a better estimate of the MLD than persistence after a couple of days. The second is that, after 2–3 d, a mixed-layer hindcast initialized from climatology shows almost the same rms MLD error as a hindcast initialized from an observed profile.

Both of these results are due to the high variability of MLD on daily time scales, and the rapid response of the mixed layer to the atmospheric forcing. For the conditions under which MILE was conducted, local hindcasts of MLD longer than a couple of days are, on average, more of a forced problem than an initial value problem. The qualification that this holds true only in an average sense must be made because there are certainly times, e.g., during the erosion of the thermocline by strong winds and surface cooling, when the evolution of the MLD is heavily dependent on the existing stratification.

Because the MLD tends to adjust to the atmospheric forcing during the heating season, the predicted near-surface stratification becomes less dependent on its initial value as the length of the hindcast is increased. Hence, the hindcast becomes less sensitive to errors in its initial conditions. (In general, of course, it is best to start with as accurate a profile as possible since the mixed-layer hindcast will have little effect on the initial profile below the maximum depth of mixing during the hindcast.) A useful result of this, as demonstrated in Fig. 4, is that the near-surface stratification of a climatological profile, or some other approximation to the existing thermal structure, can generally be improved by mixed-layer hindcasting.

Figure 5 shows a plot of rms MLD error versus time for hindcasts with the Papa data for the month of August. The results are similar to those obtained with the MILE data in Fig. 4. The hindcast error exceeds the climatological error after about 1.5 d, and the rms MLD error for hindcasts initialized from climatology is similar to the error for hindcasts initialized from an observed BT after about 2.5 d. The level of the hindcast and persistence errors for hindcasts of less than 36 h is higher than for the MILE data, which reflects the lower accuracy of the Papa data.

Figure 6 shows plots of rms MLD error versus time at Papa similar to that in Fig. 5 for all months of the year. The results for May through September are qualitatively similar to the results for August. The persistence rms error for MLD exceeds the climatological error after 1–3 d, and the error for a hindcast initialized from a climatological profile is about the same as the error for a hindcast initialized from an observed profile within 1–3 d. Hindcasts initialized from a climatological profile during the cooling season in fall and winter show significantly less skill than in spring and summer.

Table 4 — Summary of Mean and rms SST, MLD, and SCD Errors for Hindcasts of 12- and 36-h Duration Made with Data from Papa. The Errors are Calculated on a Seasonal and Annual Basis. The Model Hindcast Error is Compared with the Error for Climatology and Persistence. Model Skill is the Percent Improvement of the Model Hindcast rms Error Over the Persistence rms Error.

		SST			MLD			SCD		
Season	Model	Mean (°C)	rms (°C)	Skill	Mean (m)	rms (m)	Skill	Mean (m)	rms (m)	Skill
12-h Hindcasts										
Winter	Climate	0.08	0.51		−4.7	37.8		−15.2	36.1	
	Persistence	0.00	0.19		0.3	35.4		−0.1	24.8	
	Hindcast	0.01	0.18	1%	7.0	31.6	11%	−2.8	24.1	3%
Spring	Climate	0.06	0.54		3.3	28.1		−12.3	36.5	
	Persistence	−0.03	0.29		0.5	28.3		0.5	28.8	
	Hindcast	0.03	0.25	14%	1.3	21.2	25%	−2.2	26.5	8%
Summer	Climate	−0.12	0.93		0.0	9.7		−6.7	14.2	
	Persistence	−0.02	0.30		−0.2	8.7		−0.4	10.9	
	Hindcast	0.03	0.26	14%	−1.3	6.7	22%	−0.9	8.3	24%
Fall	Climate	0.23	0.77		−2.8	15.3		−4.3	16.8	
	Persistence	0.02	0.29		0.1	13.2		0.3	14.0	
	Hindcast	0.02	0.28	1%	0.2	11.8	11%	−0.9	12.9	8%
Annual	Climate	0.04	0.73		−0.7	23.8		−9.3	26.9	
	Persistence	−0.01	0.28		0.1	22.7		0.1	20.4	
	Hindcast	0.02	0.25	9%	1.3	18.9	17%	−1.6	18.8	8%
36-h Hindcasts										
Winter	Climate	0.05	0.51		−4.0	38.2		−14.6	36.1	
	Persistence	0.00	0.20		1.3	38.4		0.0	25.7	
	Price	−0.02	0.20	2%	10.0	33.7	12%	−2.2	24.1	6%
Spring	Climate	0.06	0.54		3.8	27.8		−11.9	36.4	
	Persistence	−0.09	0.38		1.9	32.3		2.0	31.0	
	Price	0.05	0.32	16%	0.1	21.6	33%	−2.2	27.4	12%
Summer	Climate	−0.13	0.92		0.0	9.7		−6.8	14.3	
	Persistence	−0.07	0.39		−0.3	10.2		−0.5	12.4	
	Price	0.07	0.32	19%	−2.2	7.2	29%	−1.1	8.6	31%
Fall	Climate	0.21	0.75		−2.2	15.7		−3.7	16.8	
	Persistence	0.08	0.32		−0.1	14.5		0.0	15.2	
	Price	0.03	0.30	5%	0.9	12.3	15%	0.5	13.4	12%
Annual	Climate	0.02	0.73		−0.2	23.8		−9.0	27.0	
	Persistence	−0.03	0.34		0.6	25.3		0.4	21.9	
	Price	0.04	0.29	14%	1.4	19.8	22%	−1.3	19.2	12%

The persistence rms MLD error for the MILE data in Fig. 4 decreases slightly between 4 and 5 d. This is due to the short duration of the MILE data and to the fact that fewer cases were used to calculate the error statistics for the longer hindcasts. For a normal distribution of the error, the persistence error would be expected to asymptote to a value about 1.4 times the mean (climatological) error.

The hindcast rms MLD error for the MILE data (Fig. 4) increases steadily as the duration of the hindcasts is increased. This increase is in contrast to the hindcast rms MLD error for the Papa data (Fig. 5), which increases very little. The increase in the hindcast MLD error for the MILE data with time appears to be due to a deep bias in the hindcast MLD, which can be seen in the mean hindcast error in Table 3. This bias could be due to a bias in the mixed-layer model or the atmospheric forcing or could be caused by advection.

The bias in the hindcast MLD in spring and summer for the Papa data is surprisingly small (Table 4), which means that the bias in the surface forcing and model-predicted MLD are both small or that these biases tend to cancel. There is a significant deep bias in the hindcast MLD in the winter (Table 4). This bias was noted previously at Papa and Victor (Martin 1994), and is attributed to the generation of shallow mixed layers in winter by advection of warmer water near the surface. The single-site, mixed-layer hindcasts cannot predict the formation of these shallow mixed layers, but they can deepen them once they have formed, and this contributes to the skill that the mixed-layer hindcasts exhibit during the winter (Table 4, Fig. 6).

VI. RESULTS OF THE HINDCASTS FOR ADR

Errors in hindcasting acoustic detection range were determined by calculating transmission loss from the temperature profiles with the Passive Raymode (Version 5) and split-step PE acoustic models. The temperature profiles from MILE and Papa were extended to the bottom with climatology (Beatty 1977) and were combined with climatological salinity profiles (Beatty 1977) to calculate sound speed. From the transmission loss versus range curves, the range was found at which

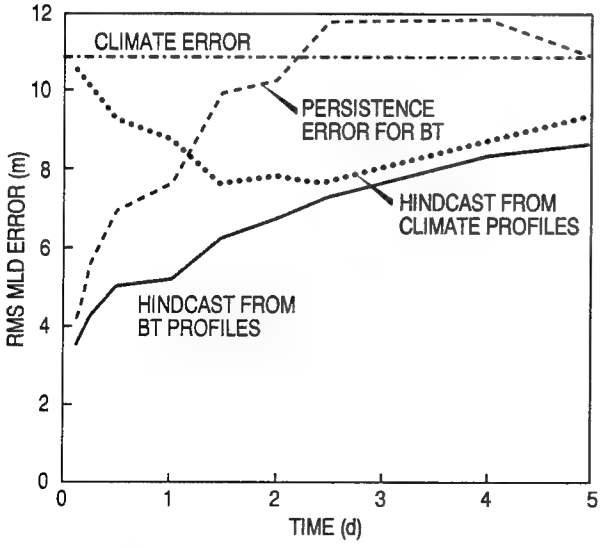

Fig. 4 — The rms MLD error versus time for the mixed-layer hindcasts with the MILE data. The rms MLD error is shown for hindcasts initialized from an observed temperature profile and from a climatological profile, and for persistence and climatology.

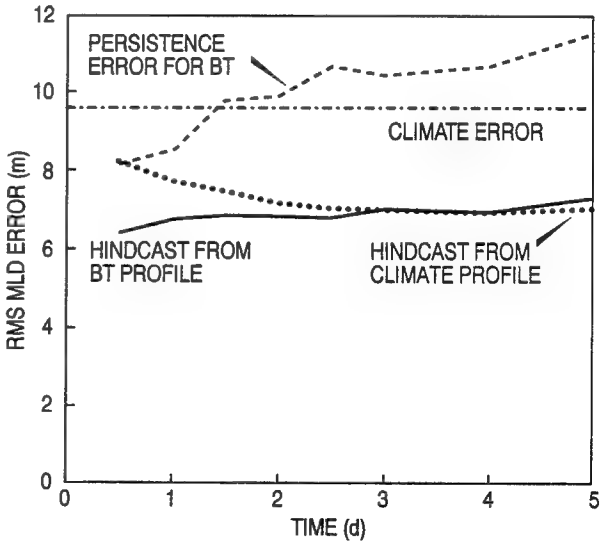

Fig. 5 — The rms MLD error versus time for the mixed-layer hindcasts with the Papa data for the month of August, calculated with data from the years 1960–1968. The rms MLD error is shown for hindcasts initialized from an observed temperature profile and from a climatological profile, and for persistence and climatology.

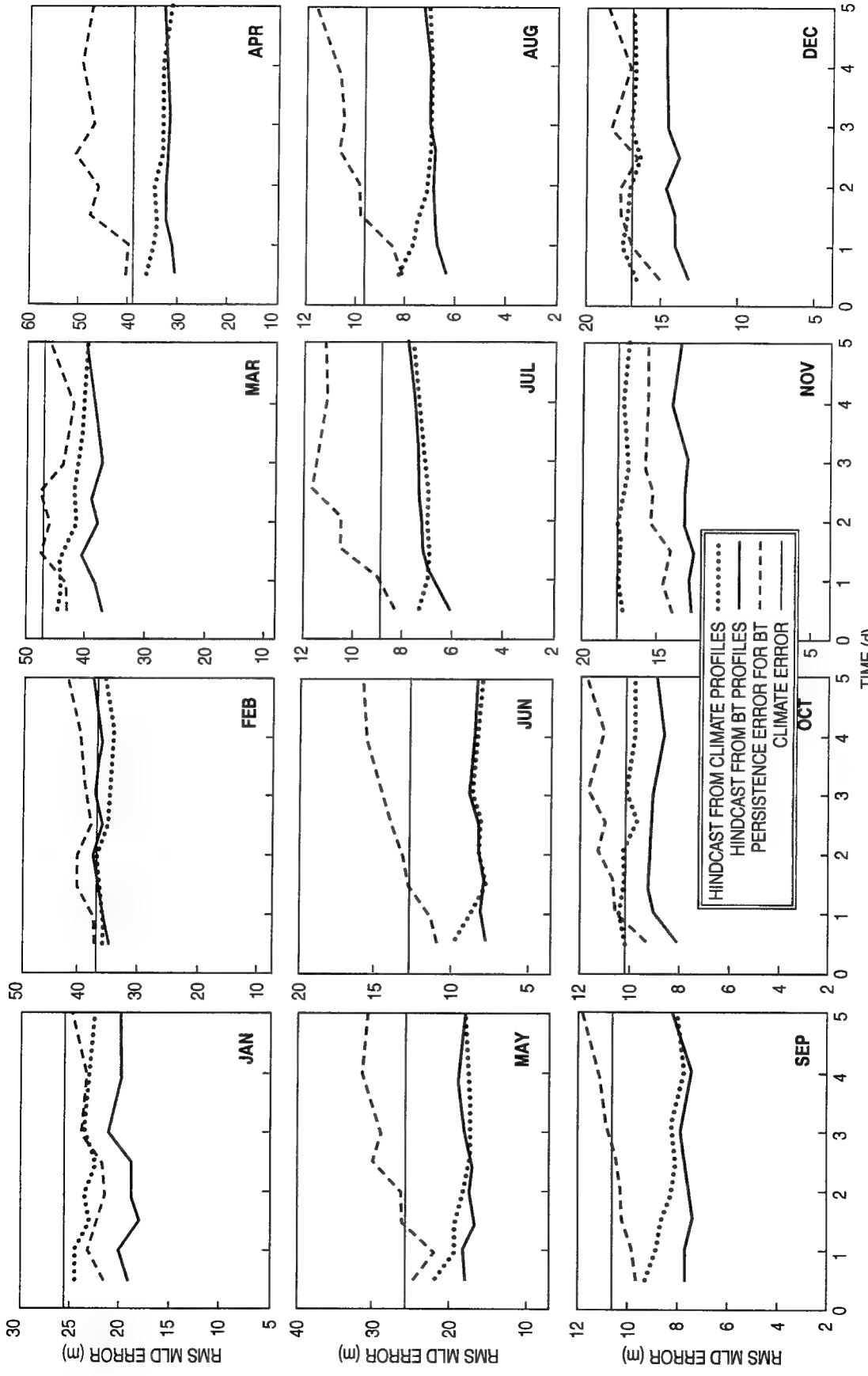

Fig. 6 — Rms MLD error versus time for mixed-layer hindcasts with data from Papa as in Fig. 5, but for all the months of the year

the transmission loss first exceeded 80 dB, and this is referred to here as the ADR. This level of transmission loss is usually reached before the first convergence zone, and provides a fairly good indication of how well the acoustic signal is being transmitted in the upper ocean, i.e., how well it is being ducted at a given frequency. Note that all the calculations of ADR with the MILE data used the MILE temperature values that were smoothed at each depth with a 2-h running mean.

Previous calculations of mixed-layer hindcast skill for ADR with data from November, Papa, and Victor (Martin 1994) utilized the Passive Raymode acoustic model. Passive Raymode was used because it calculates transmission loss very quickly, and the calculation of hindcast errors for ADR with the ocean station data involved many thousands of acoustic calculations. Since Passive Raymode is an official Navy-Standard acoustic model, it was deemed an acceptable choice. However, because of the many approximations that it makes, Passive Raymode is expected to be less accurate and less consistent in its calculations than acoustic models that directly solve the wave equation for sound propagation in the ocean, such as the PE model. The more accurate acoustic models such as the PE model, however, require much more computer time. Martin (1993) compared Passive Raymode with the PE model for some simple surface ducting situations. Although there were some notable differences for these idealized cases, the two models generally gave qualitatively similar results.

For this study, calculations of ADR with the MILE data were made with both the PE and Passive Raymode acoustic models. Using the PE model for calculating transmission loss is more feasible with the MILE data than with the ocean station data because far fewer acoustic calculations are involved. The comparison of the Passive Raymode and PE models here differs from that in Martin (1993) in that this comparison involves realistic upper-ocean sound speed profiles and includes cross-duct, as well as in-duct and below-duct source and receiver locations.

To speed up the transmission loss calculations with the PE model, a totally absorbing bottom was placed at 92-m depth. Hence, the effect of bottom reflections and convergence zones (the latter due to upward refraction of sound energy at depth caused by increasing pressure) are not accounted for. This approximation is satisfactory for this study because the interest here is only in the effect of changes in the near-surface stratification on sound propagation. Figure 7 shows a comparison of transmission loss calculated with the PE model for a totally absorbing bottom placed at depths

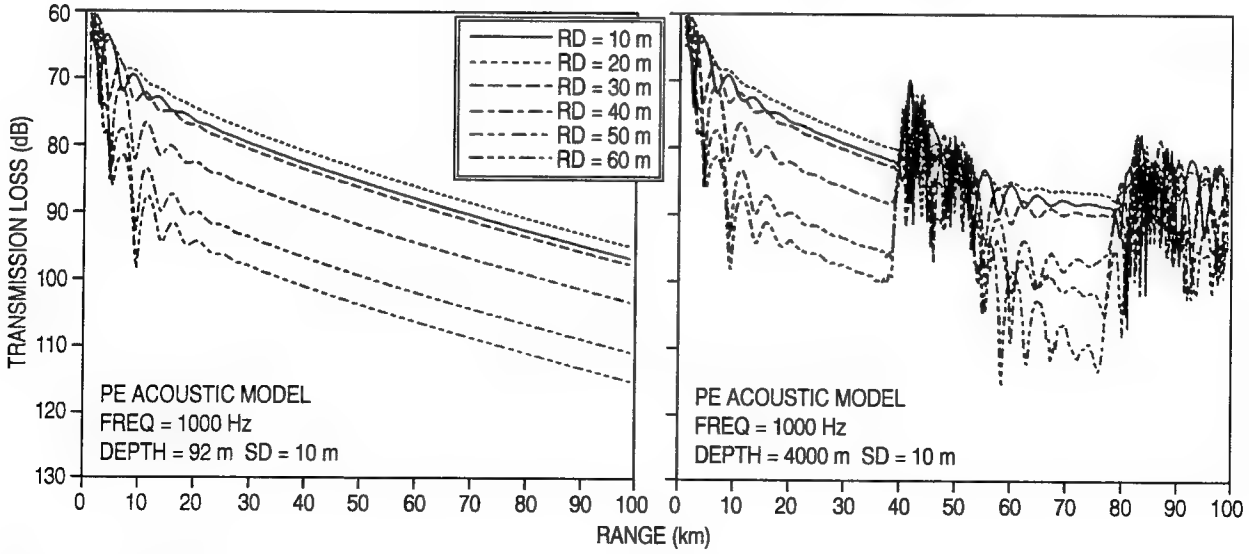

Fig. 7 — Comparison of transmission loss calculated with the PE acoustic model for a totally absorbing bottom at 92 m and 4000 m. The sound speed profile has a surface sound channel depth of 50 m. Each of the calculations is done for several source depths (SD) and receiver depths (RD).

of 92 and 4000 m for a sound speed profile with a surface sound-channel depth of 50 m and a structure below 50 m typical of the region around Papa in the summer. The transmission loss for the two sets of curves is about the same up to the first convergence zone, which occurs at a range of 40 to 55 km. Hence, the neglect of convergence from deep sound refraction will not have much of an effect on the ADRs for the MILE data, which are almost always less than 30 km.

For the calculation of ADR with the PE model, the transmission loss curves were smoothed with a 5-km running mean to filter out the fluctuations caused by the interference effects of sound signals arriving at the receiver by different paths. These fluctuations can be seen in the transmission loss curves in Fig. 7. The filtering makes the ADR values less sensitive to small variations in the transmission loss curves and more representative of the mean sound energy at a given depth.

Figures 8 and 9 show ADR calculated from the observed MILE temperature profiles at frequencies of 1000, 2000, and 4000 Hz with the PE and Passive Raymode acoustic models. The source and

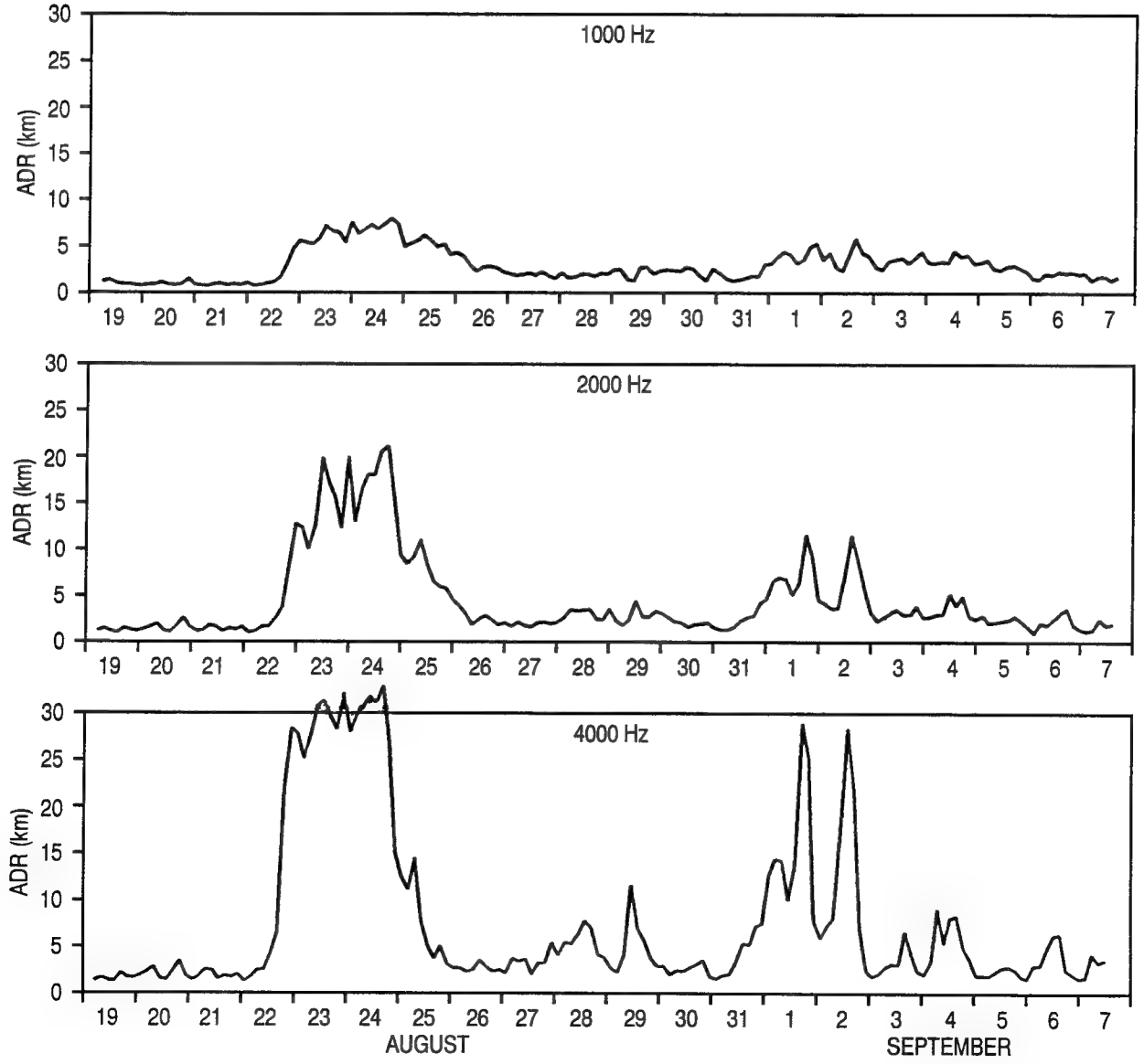

Fig. 8 — ADR during MILE calculated with the PE acoustic model for frequencies of 1000, 2000, and 4000 Hz. The source and receiver were at a 10-m depth.

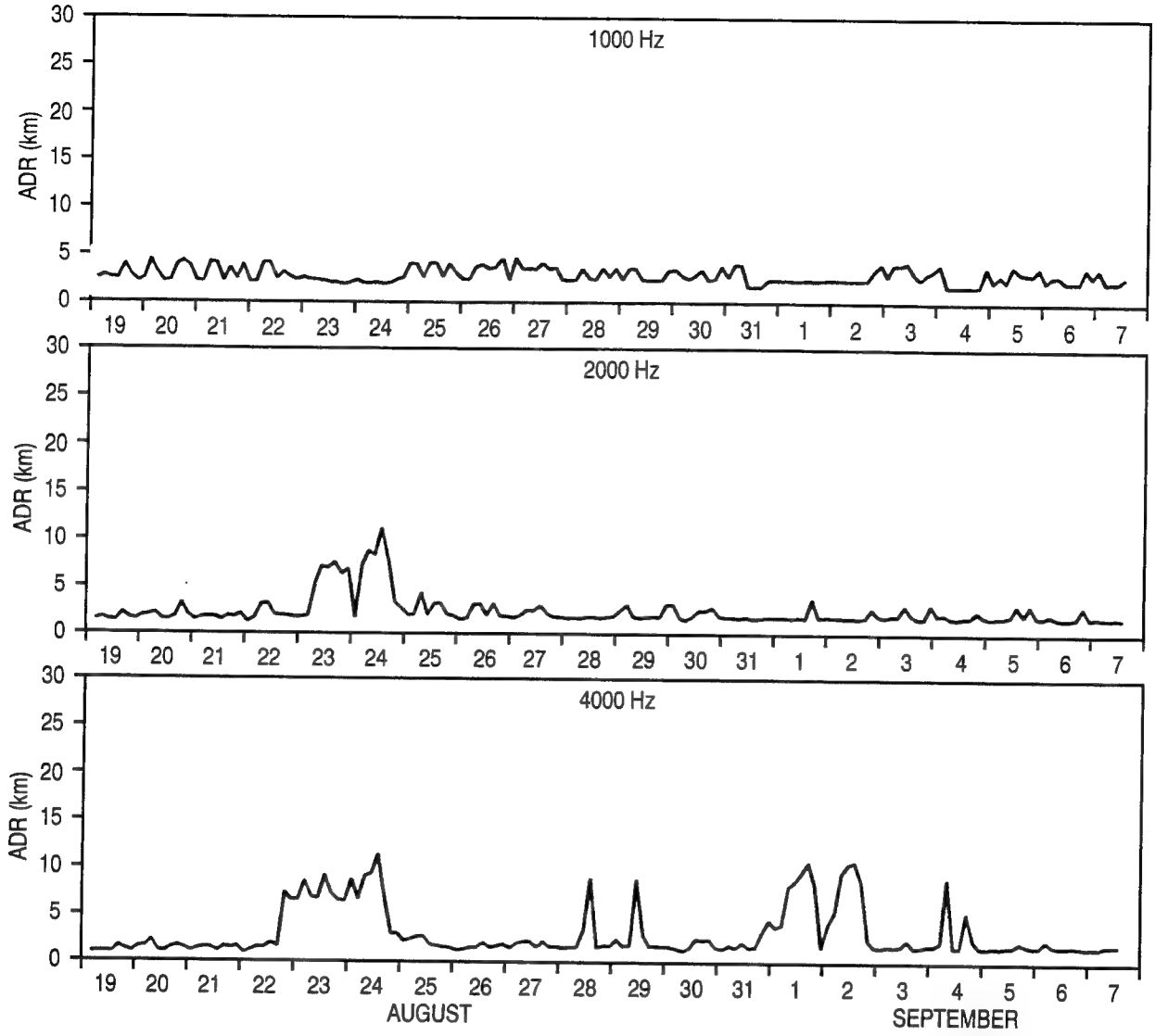

Fig. 9 — ADR during MILE calculated with the Passive Raymode acoustic model for frequencies of 1000, 2000, and 4000 Hz. The source and receiver were at a 10-m depth.

receiver were located at 10-m depth for this calculation so that the ADR values would be fairly strongly affected by changes in the depth of the surface sound channel. The PE model (Fig. 8) shows ADR increasing significantly during the periods when the surface mixed layer was deepened by strong winds. A comparison of ADR in Fig. 8 with the surface wind stress and MLD during MILE in Fig. 1 shows the strong correlation of ADR with the wind stress and MLD. Passive Raymode (Fig. 9) predicts smaller values of ADR than the PE model, and shows negligible ducting at 1000 Hz and ducting at 2000 Hz only during the strong wind event of 23–24 August. Both acoustic models predict larger values of ADR during the strong wind events as the frequency of the sound is increased. This is because the higher frequencies are more strongly ducted in the relatively shallow sound channels (less than 30 m) generated during these wind events.

Table 5 shows a summary of mean and rms ADR errors for 12- and 36-h hindcasts made with the MILE data. Results are shown for calculations of ADR with both the PE and Passive Raymode acoustic models for frequencies of 1000, 2000, and 4000 Hz for a source and receiver at 10-m

Table 5 — Summary of Mean and rms ADR Errors for 12- and 36-h Hindcasts Made with MILE Data. ADR was Calculated for a Source and Receiver at a 10-m Depth. The Model Hindcast Error is Compared with the Errors for Persistence and Climatology. Model Skill is the Percent Improvement of the Model Hindcast rms Error Over the Persistence rms Error. Results are shown for Both the PE and Passive Raymode Acoustic Models.

Hindcast Duration (h)	Model	1000 Hz			2000 Hz			4000 Hz		
		Mean (km)	rms (km)	Skill	Mean (km)	rms (km)	Skill	Mean (km)	rms (km)	Skill
Results with PE Acoustic Model										
12	Climate	0.92	1.97		1.56	4.80		2.73	9.17	
	Persistence	–0.01	1.11		–0.02	3.17		–0.05	7.05	
	Hindcast	0.01	0.85	23%	0.52	2.47	22%	1.23	4.84	31%
36	Climate	0.81	1.90		1.38	4.79		2.41	9.20	
	Persistence	–0.06	2.09		–0.08	5.84		–0.15	11.90	
	Hindcast	0.16	1.16	44%	1.04	3.61	38%	2.37	6.83	43%
Results with Passive Raymode Acoustic Model										
12	Climate	–0.24	0.80		–0.56	1.63		–0.92	2.78	
	Persistence	0.01	0.92		0.00	1.75		–0.02	2.89	
	Hindcast	–0.31	0.88	5%	–0.05	1.72	2%	0.32	1.77	39%
36	Climate	–0.24	0.80		–0.60	1.68		–1.01	2.85	
	Persistence	0.01	1.13		–0.03	2.28		–0.03	3.88	
	Hindcast	–0.40	0.90	21%	0.10	1.91	16%	0.88	2.40	38%

depth. The calculations with both acoustic models indicate that the mixed-layer hindcasts with the MILE data demonstrate skill in predicting changes in ADR. However, the results with the PE model show more consistent levels of skill than the results with Passive Raymode. The hindcast skill for ADR is 23 to 44% with the PE model versus 2 to 39% with Passive Raymode. The skill levels predicted by Passive Raymode at 1000 and 2000 Hz (2 to 21%) are much lower than the levels predicted at 4000 Hz (38 to 39%), and this is in large part due to the fact that Passive Raymode predicts little ducting at these frequencies during MILE (Fig. 9).

Errors for ADR at Papa are shown in Table 6 for hindcasts of 12- and 36-h duration. ADR was calculated with Passive Raymode for frequencies of 250, 1000, and 4000 Hz for a source and receiver at 20-m depth. As with SST, MLD, and SCD, the level of skill in hindcasting ADR shown with the Papa data is generally higher in the spring and summer than in the fall and winter, and is lower than that calculated with the MILE data. Some skill is indicated in hindcasting ADR at 250 Hz, although it tends to be lower than the hindcast skill shown at the higher frequencies. Hindcast skill for ADR at Papa in spring and summer for frequencies of 1000 and 4000 Hz ranges from 9 to 21%.

Tables 7 and 8 show hindcast skill for ADR at 1000 and 4000 Hz for 12-h hindcasts with the MILE data for a number of source and receiver depths. (Only one result is presented for each

Table 6 — Summary of Mean and rms ADR Errors for Hindcasts of 12- and 36-h Duration Made with Data from Papa. The Passive Raymode Acoustic Model was Used to Calculate ADR for a Source and Receiver at a 20-m depth. The Errors are Calculated on a Seasonal and Annual Basis. The Model Hindcast Error is Compared with the Error for Persistence. Model Skill is the Percent Improvement of the Model Hindcast rms Error Over the Persistence rms Error.

		250 Hz			1000 Hz			4000 Hz		
Season	Model	Mean (km)	rms (km)	Skill	Mean (km)	rms (km)	Skill	Mean (km)	rms (km)	Skill
12-h Hindcasts										
Winter	Persistence	0.2	16.6		0.0	12.6		0.0	4.0	
	Hindcast	−4.0	17.4	−5%	−3.5	12.7	−1%	−1.0	3.7	7%
Spring	Persistence	0.2	8.6		0.1	9.9		0.1	3.5	
	Hindcast	−1.3	8.3	3%	−2.5	8.8	12%	−0.8	3.2	9%
Summer	Persistence	0.0	1.1		−0.1	4.7		0.0	1.7	
	Hindcast	0.0	1.0	7%	−0.9	4.1	12%	−0.4	1.5	10%
Fall	Persistence	0.0	11.2		0.1	9.1		0.0	3.1	
	Hindcast	−2.7	11.3	−1%	−3.9	9.6	−5%	−0.8	3.1	0%
Annual	Persistence	0.1	9.3		0.0	9.1		0.0	3.1	
	Hindcast	−2.0	9.5	−2%	−2.7	8.8	3%	−0.7	2.9	6%
36-h Hindcasts										
Winter	Persistence	0.5	17.7		−0.2	13.6		−0.1	4.0	
	Hindcast	0.5	18.2	−2%	−1.2	13.1	4%	−0.9	3.6	11%
Spring	Persistence	0.4	9.4		0.5	11.1		0.3	3.8	
	Hindcast	−0.6	8.2	12%	−1.9	8.8	21%	−0.7	3.2	15%
Summer	Persistence	0.0	1.1		−0.1	4.8		0.0	1.8	
	Hindcast	0.0	1.0	16%	−0.7	4.1	15%	−0.3	1.5	19%
Fall	Persistence	0.0	10.9		−0.1	9.7		0.0	3.2	
	Hindcast	−1.3	10.7	2%	−2.0	9.5	2%	−0.7	3.2	1%
Annual	Persistence	0.2	9.8		0.0	9.8		0.0	3.2	
	Hindcast	−0.4	9.5	3%	−1.4	8.9	10%	−0.7	2.9	11%

source-receiver depth combination, since these acoustic calculations are symmetric, i.e., switching the locations of the source and receiver gives the same result.) Results were calculated with both the PE and Passive Raymode acoustic models. The results with the PE model are very consistent. The hindcast ADR shows skill for all the source and receiver depths tested at both 1000 and 4000 Hz, with a range of hindcast skill of 7 to 35%. The skill for the hindcast ADR is generally higher when either the source or the receiver is near the surface, which might be expected, since

Table 7 – The Skill of Hindcasting ADR with Data from MILE for Several Source and Receiver Depths for a Frequency of 1000 Hz, Calculated with Both the PE and Passive Raymode Acoustic Models. The Mixed-Layer Hindcasts were of 12-h Duration.

Source Depth (m)	Receiver Depth (m)					
	10	20	30	40	50	60
Acoustic Model = Split-Step PE						
10	23%					
20	19%	16%				
30	22%	14%	11%			
40	26%	18%	15%	21%		
50	23%	17%	19%	18%	14%	
60	25%	19%	17%	18%	10%	8%
Acoustic Model = Passive Raymode						
10	5%					
20	20%	17%				
30	–3%	0%	0%			
40	7%	15%	0%	–3%		
50	–15%	19%	–15%	0%	–4%	
60	0%	16%	–7%	–6%	9%	–1%

the mixed-layer hindcasts predict only changes in the sound-speed gradient near the surface. As the depths of both the source and receiver are increased, the hindcast skill for ADR tends to decrease.

The results with the Passive Raymode acoustic model are not nearly as consistent as with the PE model, especially at 1000 Hz. As noted previously, Passive Raymode predicts negligible ducting and, hence, small values of ADR at 1000 Hz (Fig. 9), and the variability of hindcast skill for ADR calculated with Passive Raymode at this frequency suggests that the variability in ADR that does exist at 1000 Hz is somewhat random. The results with Passive Raymode are significantly better at 4000 Hz than at 1000 Hz but are not as consistent as the results with the PE model at 4000 Hz, especially when both the source and receiver are located below 30 m. This inconsistency suggests that Passive Raymode has trouble predicting transmission loss for these cases of below-duct sound propagation.

Table 9 shows the improvement over persistence for rms ADR error for mixed-layer hindcasts at Papa of 24-h duration for spring and summer for several source and receiver depths. The results show skill in hindcasting ADR when both the source and receiver are located in the upper 30 m, but little or no skill when either the source or the receiver is located at 60 m. Again, the poor results with the source or receiver at 60-m depth suggest that Passive Raymode may have trouble predicting transmission loss for cross- and below-duct sound propagation.

Table 8 — The Skill of Hindcasting ADR with Data from MILE for Several Source and Receiver Depths for a Frequency of 4000 Hz, Calculated with Both the PE and Passive Raymode Acoustic Models. The Mixed-Layer Hindcasts were of 12-h Duration.

Source Depth (m)	Receiver Depth (m)					
	10	20	30	40	50	60
Acoustic Model = Split-Step PE						
10	31%					
20	35%	9%				
30	28%	19%	7%			
40	27%	23%	10%	14%		
50	26%	23%	17%	15%	23%	
60	26%	23%	14%	16%	25%	15%
Acoustic Model = Passive Raymode						
10	39%					
20	12%	25%				
30	15%	18%	0%			
40	13%	22%	7%	−3%		
50	20%	23%	11%	−7%	−6%	
60	21%	27%	12%	−3%	−9%	−54%

Table 9 — The Skill of Hindcasting ADR with Data from Papa for Several Source and Receiver Depths for a Frequency of 1000 Hz, Calculated with the Passive Raymode Acoustic Model. The Mixed-Layer Hindcasts were of 24-h Duration.

Source Depth (m)	Receiver Depth (m)			
	10	20	30	60
Spring				
10	15%			
20	16%	16%		
30	15%	16%	15%	
60	2%	0%	1%	2%
Summer				
10	14%			
20	15%	15%		
30	11%	12%	11%	
60	0%	−2%	0%	7%

VII. SUMMARY

The skill of short (less than 5 d) duration mixed-layer hindcasts was investigated with data from MILE and from Ocean Weather Station Papa. Papa was located in the northeast Pacific at 50° N, 145° W. The Papa data used here cover a 9-yr period from 1960 to 1968. MILE was conducted about 40 km southwest of Papa over a 20-d period in August and September of 1977. These two data sets offer a useful contrast in that the Papa data consist of many years of meteorological and bathythermograph observations that allow investigation of seasonal and interannual variations for a wide range of conditions, whereas the MILE observations are more extensive and accurate, but cover only a short period.

A number of previous mixed-layer hindcast studies have utilized the MILE and Papa data (Martin 1988, 1989, 1993, 1994). The purpose of this study was to perform a more detailed comparison of hindcast skill with the two data sets and to investigate several questions that had not been considered before, notably: how do hindcast and persistence errors compare with climatological errors, what is the hindcast skill for acoustic propagation with the MILE data, and how do the Passive Raymode and PE acoustic models compare in calculating hindcast errors for acoustic propagation with the MILE data.

The hindcasts with the MILE and Papa data were initialized and validated with observed temperature profiles and forced with surface wind stresses and heat fluxes calculated from meteorological observations. Mean and rms hindcast errors for SST, MLD, SCD, and ADR were compared with errors for persistence and climatology. Hindcast skill was calculated as the percent improvement of the hindcast rms error over the persistence rms error. ADR is defined as the range at which the transmission loss at a given frequency first exceeds 80 dB.

The hindcasts with the MILE and Papa data showed skill relative to persistence. The hindcast skill was significantly higher with the MILE data than with the Papa data. The hindcasts at Papa generally showed more skill in spring and summer than in fall and winter. The range of hindcast skill for hindcasts of 12- to 36-h duration in spring and summer was 39 to 48% for SST, 28 to 37% for MLD, and 38 to 43% for SCD with the MILE data and 14 to 19% for SST, 22 to 33% for MLD, and 8 to 31% for SCD with the Papa data. Smoothing the MILE temperature observations with a 2-h running mean increased the hindcast skill about 3% over the values obtained with the unsmoothed data due to a reduction of the small-scale noise.

For SST, the climatological rms error was almost always greater than the hindcast or persistence rms error. This might be expected due to year-to-year variations in the ocean temperature. However, for MLD the persistence rms error was found to generally exceed the climatological error after about 2 d during the spring and summer, i.e., after 2 d the climatological MLD was a better estimate of the actual MLD than persistence. This illustrates the high temporal variability of the MLD coupled with the fact that the MLD tends to occupy a similar range from year-to-year during the heating season.

Because of the high variability of MLD during the heating season and the rapid changes in MLD in response to changes in the atmospheric forcing, hindcasts initialized from a climatological temperature profile showed skill for MLD similar to that for hindcasts initialized from an observed profile for hindcasts longer than about 2 d. The fact that the near-surface stratification of climatological estimates of ocean thermal structure can be improved by mixed-layer hindcasting is a very useful result for operational upper-ocean prediction.

Hindcast and persistence errors for ADR (defined as the range at which the transmission loss first exceeds 80 dB) were calculated for the MILE data with both the PE and Passive Raymode acoustic models for frequencies of 1000, 2000, and 4000 Hz for a source and receiver depth of 10 m. The range of hindcast skill for ADR was 22 to 44% for the PE model and 2 to 39% for Passive Raymode. ADR errors were calculated for the Papa data with Passive Raymode for frequencies of 250, 1000, and 4000 Hz for a source and receiver depth of 20 m. As for SST, MLD, and SCD, skill for hindcasts of ADR with the Papa data was generally higher in spring and summer than in fall and winter and was lower than for the MILE data.

The calculation of hindcast skill for ADR with the MILE and Papa data showed a general decrease in skill as the depths of both the source and receiver were increased. For a fixed source depth, however, the hindcast skill for ADR calculated with the MILE data with the PE model did not change greatly as the receiver depth was varied between 10 and 60 m (and vice versa).

Comparisons of skill in hindcasting ADR during MILE, determined from transmission-loss calculations with the Passive Raymode and PE acoustic models, showed generally higher levels of skill and more consistent results with the PE model, especially for cases where ducting was marginal, or where the source and receiver were below 30 m, which was the maximum depth of the surface mixed layer during MILE.

VIII. CONCLUSIONS

Taken together, the results with the MILE and Papa data suggest that mixed-layer hindcasting can provide a useful estimate of changes in SST and stratification caused by atmospheric forcing in the northeast Pacific. The results with the MILE data indicate that the skill for mixed-layer hindcasts of SST and MLD can be quite high, i.e., 30 to 50%. Of course, a drawback of the estimates of hindcast skill with the MILE data is that they are based on a short data set and, hence, on a limited set of conditions. The Papa hindcast results, however, which are based on many years of data and should be fairly reliable, provide estimates of hindcast skill for the spring and summer seasons that are certainly significant: 14 to 19% for SST and 22 to 33% for MLD. Since the MILE data are of better quality, a good part of the difference in hindcast skill estimated with the MILE and Papa data might be attributed to the difference in the accuracy of the observations. Estimates of hindcast skill for upper-ocean thermal structure with additional data sets of high quality would help to determine the upper limits of skill that can be expected for mixed-layer hindcasting in different regions and under different conditions.

The variability of MLD during the heating season in spring and summer at OWS Papa is such that a persistence estimate of MLD is less reliable than climatology after about 2 d. This is likely true for large areas of the ocean and is due to the rapid adjustment of the mixed layer to diurnal and day-to-day fluctuations in the atmospheric forcing. A consequence is that a hindcast of MLD longer than a day or two during the heating season is not especially sensitive to its initial conditions. (This is true, of course, only in an average sense. For a situation where the initial stratification is eroded by wind-driven or convective mixing, the MLD will be, to some degree, dependent on the initial stratification.) This situation is advantageous for operational needs, since the near-surface stratification of estimates of ocean thermal structure from such sources as satellite surface observations and historical data can be improved by mixed-layer hindcasting by utilizing the hindcasts to bring the MLD and near-surface stratification into adjustment with recent atmospheric forcing.

Atmospheric forcing can be acquired from direct observations. However, for large-scale implementation, atmospheric forcing must be obtained from operational analyses and forecasts such as those generated at the Fleet Numerical Meteorology and Oceanography Center (FNMOC) by the Navy Operational Global Atmospheric Prediction System (NOGAPS). NOGAPS is currently being used at FNMOC to drive global and regional versions of the Navy's operational ocean thermal prediction model, the Thermodynamic Ocean Prediction System (TOPS). Since the atmospheric fields from NOGAPS are likely to be less accurate than the local meteorological observations used in this study, it would be useful to determine the accuracy of the NOGAPS surface winds and heat fluxes and calculate estimates of the skill of mixed-layer hindcasts that are driven by atmospheric forcing from NOGAPS.

For reasons of efficiency, Passive Raymode was used in this and in past studies to calculate transmission loss to obtain hindcast errors for ADR. In comparisons with a PE acoustic model with data from MILE, Passive Raymode gave results that were less consistent, especially for cases where ducting was marginal, or where the source and receiver were below 30 m. It appears to be desirable to use a more accurate, or at least more consistent, acoustic model than Passive Raymode to calculate transmission loss in these types of investigations when possible. However, based on the somewhat limited results here, previous calculations of hindcast skill for ADR with Passive Raymode, which used a shallow source and receiver depth of 20 m and were based on a large number of cases, should be roughly representative of results that would have been obtained with a more accurate acoustic model, but with a slight underestimate of predictive skill, overall, due to inconsistencies in the transmission loss provided by Passive Raymode.

IX. ACKNOWLEDGMENTS

This work was sponsored by the Office of Naval Research through the Battle Group Environmental Enhancement Program (Program Element 0602435N) managed by Juergen Richter, and through the Tactical Oceanography Task of the Naval Ocean Modeling and Prediction Program (Program Element 0602435N) managed by Robert Peloquin.

Thanks are extended to John Campbell and David King of NRL's Acoustic Simulation and Tactics Branch and to Robert McGirr, formerly of the Acoustic Simulation and Tactics Branch, for their help in implementing the Passive Raymode acoustic model, and to Marshall Bradley and Susan Gibson of Planning Systems, Incorporated for their help in implementing the split-step PE acoustic model.

X. REFERENCES

Beatty, W. H., "Variability of Oceanographic Conditions at Ocean Weather Stations in the North Atlantic and North Pacific Oceans," NAVOCEANO Technical Note 3700-67-77, U.S. Naval Oceanographic Office, Washington, D.C., 100 pp., 1977.

Davis, R. E., R. DeSzoeke, D. Halpern, and P. Niiler, "Variability in the Upper Ocean During MILE. Part I: The Heat and Momentum Balances," *Deep Sea Res.* **28**, 1427–1451 (1981).

Garratt, J. R., "Review of Drag Coefficients Over Oceans and Continents," *Mon. Weather Rev.* **105**, 915–929 (1977).

Jerlov, N. G., *Marine Optics* (Elsevier, New York, NY, 1976), 231 pp.

Kondo, J., "Air-Sea Transfer Coefficients in Diabatic Conditions," *Boundary-Layer Meteorology* **9**, 91–112 (1975).

Kundu, P. K., "A Numerical Investigation of Mixed-Layer Dynamics," *J. Phys. Oceanogr.* **10**, 220–236 (1980).

List, R. J., *Smithsonian Meteorological Tables*, 6th ed. (Smithsonian Institution, Washington, D.C., 1958) 527 pp.

Martin, P. J., "Simulation of the Mixed Layer at OWS N and P with Several Models," *J. Geophys. Res.* **90**, 903–916 (1985).

Martin, P. J., "Testing and Comparison of Several Mixed-Layer Models," NORDA Report 143, Naval Research Laboratory, Stennis Space Center, MS, 30 pp., 1986.

Martin, P. J., "Effect of Forcing Errors on Short Time-Scale Mixed-Layer Hindcasts at OWS Papa," Workshop Report on Atmospheric Forcing of Ocean Circulation, Institute for Naval Oceanography, Stennis Space Center, MS, 389 pp., 1988.

Martin, P. J., "Testing of a Shipboard Thermal Forecast Model II," NOARL Technical Note 3, Naval Research Laboratory, Stennis Space Center, MS, 1989.

Martin, P. J., "Sensitivity of Acoustic Transmission Loss Prediction to Mixed-Layer Hindcasts Calculated with Data from Ocean Weather Station Papa," NRL Formal Report 9426, Naval Research Laboratory, Stennis Space Center, MS, October 1993.

Martin, P. J., "Hindcasting Changes in Upper-Ocean Thermal Structure and Acoustic Transmission Loss on Short Time Scales with Data from Ocean Weather Stations November, Papa, and Victor," NRL Formal Report 9602, Naval Research Laboratory, Stennis Space Center, MS, October 1994.

Pollard, R. T., P. B. Rhines, and R. O. R. Y. Thompson, "The Deepening of the Wind-Mixed Layer," *J. Mar. Res.* **33**, 405–422 (1973).

Price, J. F., R. A. Weller, and R. Pinkel, "Diurnal Cycling: Observations and Models of the Upper Ocean Response to Diurnal Heating, Cooling, and Wind Mixing," *J. Geophys. Res.* **91**, 8411–8427 (1986).

Stull, R. B., and T. Hasegawa, "Transilient Turbulence Theory. Part II: Turbulent Adjustment," *J. Atm. Sci.* **41**, 3368–3379 (1984).

Tabata, S., "Insolation in Relation to Cloud Amount and Sun's Altitude," in *Studies in Oceanography*, Y. Kozo, ed. (University of Washington Press, Seattle, WA, 1964).

Wyrtki, K., "The Average Annual Heat Balance of the North Pacific Ocean and its Relation to Ocean Circulation," *J. Geophys. Res.* **70**, 4547–4559 (1965).